A DFT-based comparative study on the excited states intramolecular proton transfer in 1-hydroxy-2-naphthaldehyde and 2-hydroxy-3-naphthaldehyde

ARTICLE *in* JOURNAL OF MOLECULAR STRUCTURE THEOCHEM · APRIL 2007

Impact Factor: 1.37 · DOI: 10.1016/j.theochem.2006.12.010

4 AUTHORS, INCLUDING:

Sudipta Dalai
Vidyasagar University
73 PUBLICATIONS **836** CITATIONS
SEE PROFILE

Ajay Misra
Vidyasagar University
56 PUBLICATIONS **907** CITATIONS
SEE PROFILE

ELSEVIER

Journal of Molecular Structure: THEOCHEM 807 (2007) 33–41

THEO CHEM

www.elsevier.com/locate/theochem

A DFT-based comparative study on the excited states intramolecular proton transfer in 1-hydroxy-2-naphthaldehyde and 2-hydroxy-3-naphthaldehyde

Sankar Prasad De, Sankarlal Ash, Sudipta Dalai, Ajay Misra *

Department of Chemistry and Chemical Technology, Vidyasagar University, Midnapore 721 102, West Bengal, India

Received 15 November 2006; accepted 4 December 2006
Available online 13 December 2006

Abstract

Potential energy (PE) curves for the intramolecular proton transfer in the ground (GSIPT) and excited (ESIPT) states of 1-hydroxy-2-naphthaldehyde (1H2NA) and 2-hydroxy-3-naphthaldehyde (2H3NA) were studied using DFT/B3LYP(6-31G) and TD-DFT/B3LYP(6-31G) level of theory, respectively. Our calculations suggest the non-viability of ground state intramolecular proton transfer for both the compounds. Excited states PE calculations support the ESIPT process to both 1H2NA and 2H3NA. The wide difference in ESIPT emission process of 1H2NA and 2H3NA have been explained in terms of HOMO and LUMO electron density of the enol and keto tautomer of these two compounds.

Keywords: Ground state intramolecular proton transfer; Excited state intramolecular proton transfer; 1-Hydroxy-2-naphthaldehyde; 2-Hydroxy-3-naphthaldehyde; DFT; B3LYP; Potential energy

1. Introduction

Excited state intramolecular proton transfer (ESIPT) reactions are of great scientific and technological interest. Since its introduction, the photoinduced excited state intramolecular proton (or hydrogen) transfer reaction, which generally incorporate transfer of a hydroxyl (or amino) proton to the carbonyl oxygen (imine nitrogen) through a pre-existing intramolecular hydrogen bonding (IMHB) configuration, has received considerable attention, because it has led to a wide range of application, such as laser dyes [1,2], polymer stabilizer [3], Raman filters [4] environmental probes in bio-molecules [5], etc. Main requirement of ESIPT reaction is that the molecule must have acid and basic groups and the strong intramolecular hydrogen bond between the two groups at the same time. A large number of molecules belonging to this class e.g., *o*-hydroxybenzoyl [6–16], *o*-hydroxy Schiff bases [17–20] and so on.

Weller [21,22], in his pioneering work, had pointed out the dual emission in the fluorescence spectra of salicylic acid and methyl salicylate and attributed it to asymmetric double-well potential arising from proton transfer in the ground state and also in the excited states as shown in Scheme 1. The two wells in the ground state potential energy curve represent the primary (N) and tautomeric (T) forms, and the two wells in the excited state curve represent the corresponding excited states N^* and T^* respectively. It is clear from Scheme 1 that the N form is the most stable in the ground state and T^* in the excited state.

Since the original work of Weller [21] on the ESIPT of methyl salicylate (MS), a large number of experimental [23–30] and theoretical [31–37] studies on the ESIPT of a variety of systems have been reported. Among them, MS [38–44] and its related compounds, *o*-hydroxy-acetophenone (OHAP) [45–47] and *o*-hydroxy-benzaldehyde (OHBA) [48–51] have been well-studied as prototypes of

* Corresponding author. Tel.: +91 9433220206; fax: +91 3222 275329.
E-mail address: ajaymsr@yahoo.co.in (A. Misra).

0166-1280/$ - see front matter © 2006 Elsevier B.V. All rights reserved.
doi:10.1016/j.theochem.2006.12.010

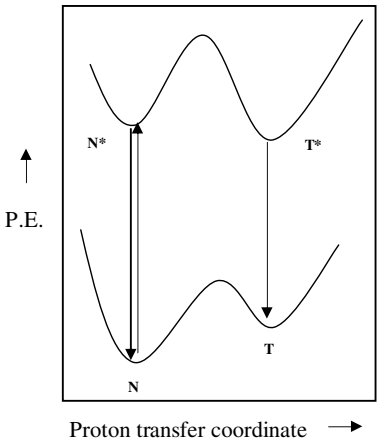

Scheme 1.

molecules showing ESIPT process. Though theoretical studies on ESIPT on MS and related compounds are quite enriched, the similar information about their naphthalene analog is not so many. Evidence on the existence of intramolecular hydrogen bond in methyl-2-hydroxy-3-naphthoate (MHN23) has been reported by Bergmann et al. [52]. Dual emission of MHN23 was first reported by Naboikin et al. [53]. MHN23 possess a strong IMHB in the ground electronic state and also shows ESIPT upon excitation to its excited singlet states. On the other hand, the lack of ESIPT emission from methyl-1-hydroxy-2-naphthoate (MHN12) and methyl-2-hydroxy-1-naphthoate (MHN21) had been explained by Catalán et al. [54], in terms of the non-radiative dynamics of their respective normal tautomers. Shizuka and co-workers [55] carried out a comprehensive study on ESIPT of 1-hydroxy-2-acetonaphthone (1H2AN), 1-hydroxy-2-naphthaldehyde (1H2NA) and methyl-1-hydroxy-2-naphthoate (1H2MN) by means of laser photolysis, time-resolved thermal lensing and fluorometry method. They found that both 1H2NA and 1H2AN show ESIPT, whereas 1H2MN gives no ESIPT emission. They also observed structured ESIPT emission band ($\lambda_{em} = 476$ nm) for 1H2NA with a very little Stokes shift. They showed that distinct relaxation properties of 1H2NA, 1H2AN and 1H2MN are responsible for the relative stabilities between parent enol ('N' form) and tautomeric keto ('T') forms in the lowest excited singlet states of these compounds. On the other hand, laser-induced fluorescence studies by Wu et al. [56] showed a weak tautomeric emission band maximized at 715 nm for 2-hydroxy-3-naphthaldehyde (2H3NA) in cyclohexane at 298 K with the fluorescence quantum yield as low as 6.8×10^{-6}. 1H2NA and 2H3NA differ only on the relative position of –OH and –CHO group, but they show wide difference in their fluorescence properties. This wide difference of fluorescence properties of these two compounds motivates us to do the present extensive quantum mechanical investigations, to get some insight in terms of their electronic structure.

Hybrid HF/DFT methods have been proposed as reliable tools for electronic computation in a general protocol for studying static and dynamic properties of hydrogen bonded systems [54,57,58]. One such method, B3LYP [59], predicts the available experimental data, as well as the results obtained with the highest post-HF method [60]. In view of its wide spread success for the calculation of large molecules [58], we decided to choose density functional approach for the present calculation of the excited state proton transfer process in 1H2NA and 2H3NA.

2. Theoretical calculations

All ab initio calculations reported in this paper were carried out using the Gaussian 03 suite programs [60]. We compared the results for a number of method and basis sets and found that the DFT-based calculations using hybrid functional (B3LYP) with 6-31G basis set to be the optimal one in terms of price–performance ratio for carrying out elaborate electronic structure calculations within our limited computational resource. Analytic vibrational frequency computations at the optimized structure were done to confirm the optimized structure to be an energy minimum or a transition structure.

Strength of the intramolecular hydrogen bond (IMHB) of each molecule studied was evaluated as the difference between the energy of the fully optimized structure of the non-hydrogen bonded form (hydroxyl group rotated by 180°) and the energy of the N-tautomer.

Ground state intramolecular proton transfer (GSIPT) curves were calculated with energies of the B3LYP/6-31G fully optimized structures at fixed O–H distances over the 0.8–2.0 Å range. Information on the ESIPT mechanism was obtained by calculating the Franck–Condon (FC) transition energies for the DFT (B3LYP)/6-31G ground state structures at the TD-DFT(B3LYP)/6-31G level. The Franck–Condon (FC) curves for the proton transfer processes were obtained by adding the TD-DFT(B3LYP)/6-31G excitation energies to the corresponding GSIPT curves.

Free energy calculations on the optimized ground state 'N' and 'T' form of both compounds were done by RHF/6-31G(d) level of theory.

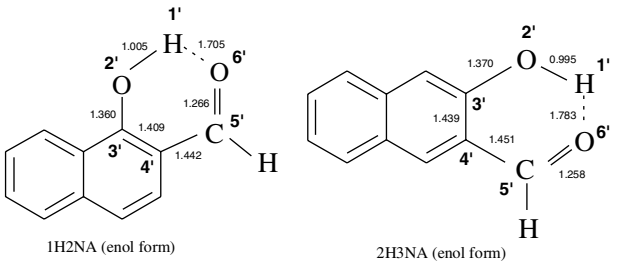

Scheme 2.

3. Results and discussion

Ground state optimized structure of both 1H2NA and 2H3NA shows that the enol form ('N' form) is the stable structure having strong intramolecular hydrogen bonding (Scheme 2). Bond length, bond angle and dihedral angle of the six-membered ring system containing intramolecular hydrogen bond of both 1H2NA and 2H3NA are given as Supplementary data with this text.

Ground state bond angle and dihedral angle data (see Supplementary data), suggest that the six member ring formed due to IMHB for both 1H2NA and 2H3NA are planar and they are in the same plane that of the naphthalene ring. A critical analysis of the bond length data shows that C(3′)–C(4′) and O(6′)–H(1′) bond is much shorter in 1H2NA than 2H3NA. Shorter O(6′)–H(1′) distance is a measure of stronger IMHB in 1H2NA. Again the double bond character at C(3′)–C(4′) in 1H2NA and single bond character at C(3′)–C(4′) in 2H3NA supports the fixed double bond character of naphthalene ring. In other words IMHB in 1H2NA will be more conjugated and hence the strength of hydrogen bonding will be more compare to 2H3NA.

In order to get some idea about the relative strength of IMHB in 1H2NA and 2H3NA, we compare the C=O and O–H stretching frequencies of these two compounds with some model compounds like, 1-naphthol, 2-naphthol and 2-naphthaldehyde (Table 1). We used B3LYP/6-31G (d) level of theory for calculation of frequencies and 0.9613 was used as scale factor for frequencies as given in [61]. Table 1 shows that our methodology for calculation of vibrational frequency works nicely, since our calculated C=O and O–H stretching frequencies agree well with the experimental results. It is reasonable to infer from both the experimental as well as theoretical calculations that the position of O–H absorption in these mono-substituted compounds (1-naphthol and 2-naphthol) is independent of substitution. Hunsberger [62] showed that for the di-substituted compounds (1H2NA and 2H3NA), the displacement of the OH band ($\Delta\nu_{OH}$) from its average position in 1-naphthol and 2-naphthol and the displacement of the C=O band ($\Delta\nu_{C=O}$) from its average position in the corresponding mono-substituted i.e. 2-naphthaldehyde are taken as a quantitative measure of the strength of IMHB in the di-substituted compounds. Greater red shift of the band positions from its mono-substituted compound i.e. larger values of $\Delta\nu_{OH}$ and $\Delta\nu_{C=O}$ are taken as evidence for corresponding stronger IMHB. Now both the experimental and theoretical data of $\Delta\nu_{OH}$ and $\Delta\nu_{C=O}$ in Table 1 suggests that 1H2NA has stronger IMHB than 2H3NA.

The strength of the intramolecular hydrogen bond of the enol form ('N') is calculated, by rotating the phenolic –OH group out of the hydrogen bonded conformation and computing the difference in energy between the closed and open form, for 1H2NA and 2H3NA are shown in Figs. 1 and 2, respectively. The calculated IMHB strength for 1H2NA and 2H3NA are found to be 17.14 and 12.34 kcal/mole, respectively. Figs. 1 and 2 also show that barrier for phenolic –OH rotation and it is found to be 19.08 kcal/mole in 1H2NA and 15.25 kcal/mole in 2H3NA. Thus the relative strength of IMHB is 5 kcal/mol more in 1H2NA than that of 2H3NA.

The conversion from 'N' to 'T' in the ground electronic state can be thought of as arising due to the transfer of proton from $O_d(2')$ to $O_a(6')$ with simultaneous redistribution of electron density within the six-membered hydrogen bonded ring. Some authors have considered the O_d–O_a distance as fixed and varied the O_d–H bond distance to get an

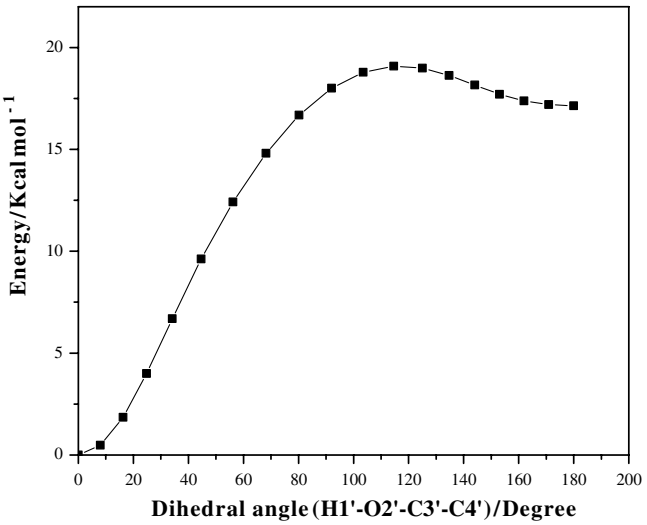

Fig. 1. Energetics of the transformation from IMHB from ('N') to the non-hydrogen bonded form (hydroxyl group rotated by 180°) of 1H2NA. For each value of dihedral angle (H(1′)–O(2′)–C(3′)–C(4′)), the geometry has been optimized using the DFT-B3LYP(6-31G) level of theory.

Table 1
Theoretical and experimental carbonyl and hydroxyl stretching frequency values of 1H2NA, 2H3NA and some model compounds

Compounds	C=O stretching frequencies (in cm^{-1})		O–H stretching frequencies (in cm^{-1})		$\Delta\nu_{C=O}$		$\Delta\nu_{O-H}$	
	Theo.	Exp.[a]	Theo.	Exp.[a]	Theo.	Exp.[a]	Theo.	Exp.[a]
α-Naphthol			3608	3618				
β-Naphthol			3609	3618				
2-Naphthaldehyde	1729	1702						
1H2NA	1654	1637	3097	3178	75	64	511	440
2H3NA	1675	1670	3280	3249	54	31	329	369

[a] Experimental values of IR frequencies (in 0.02 m CCl_4) are obtained from Ref. [62].

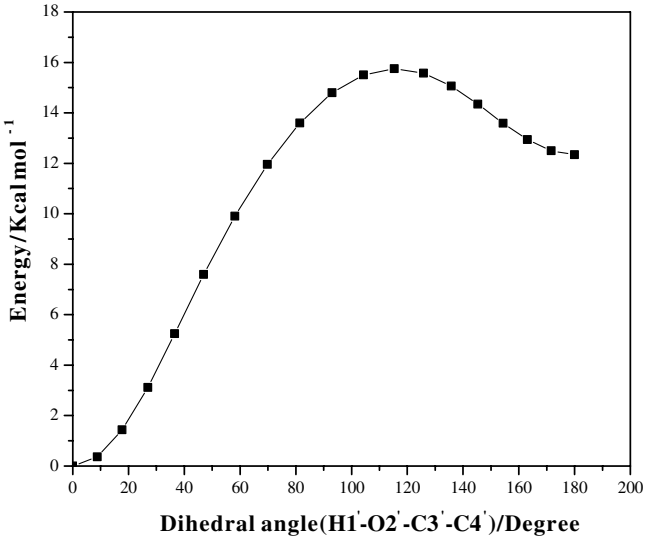

Fig. 2. Energetics of the transformation from IMHB from ('N') to the non-hydrogen bonded form (hydroxyl group rotated by 180°) of 2H3NA. For each value of dihedral angle (H(1′)–O(2′)–C(3′)–C(4′)), the geometry has been optimized using the DFT-B3LYP(6-31G) level of theory.

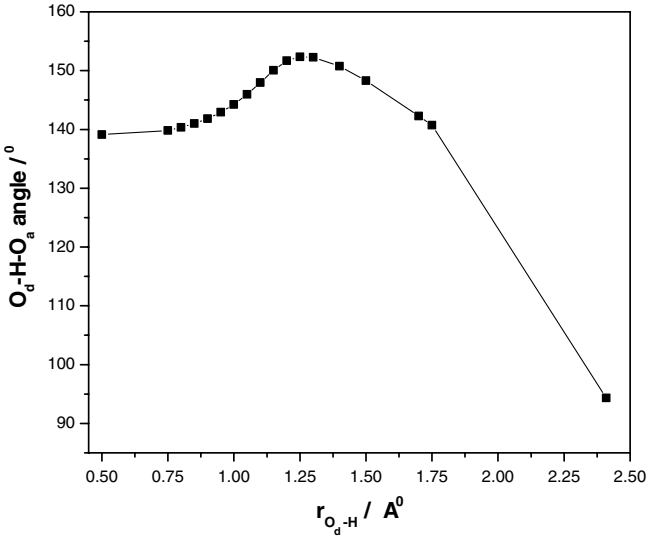

Fig. 4. Variation of O_d–H–O_a angle of 1H2NA with r_{O_d-H} as obtained from DFT-B3LYP(6-31G) level of theory.

idea about the potential energy curve for both GSIPT and ESIPT processes.

A plot of $O_d(2')$–$O_a(6')$ distance as a function of r_{O_d-H} of 1H2NA as shown in Fig. 3 revels that as the proton shifted from O_d to O_a, the O_d–O_a distance changes significantly. At smaller O_d–H distance it increases slowly. In the close vicinity of a stable O_d–H distance, the O_d–O_a distance falls sharply. But as the proton shifted further from O_d, it decreases sharply, passes through minimum and then enlarging to a distance comparable to that in the 'T' form. Fig. 4 shows the variation of O_d–H–O_a angle as a function of r_{O-H} distance. At smaller O_d–H distance, it increases slowly. The O_d–H–O_a angle increases sharply in the near vicinity of the stable O_d–H distance. Then increases with the increase of r_{O-H} distance, reaches maximum and then shows a sudden fall with the further increases of r_{O-H} distance. We obtain similar variation of $r_{O_d-O_a}$ and O_d–H–O_a angle with r_{O_d-H} in case of 2H3NA. Therefore, it becomes clear that by freezing the geometry or by fixing the O_d–O_a distance at a particular values, one ends up introducing artificial constraints on the system and hence a barrier for the enol (N) to keto (T) conversion.

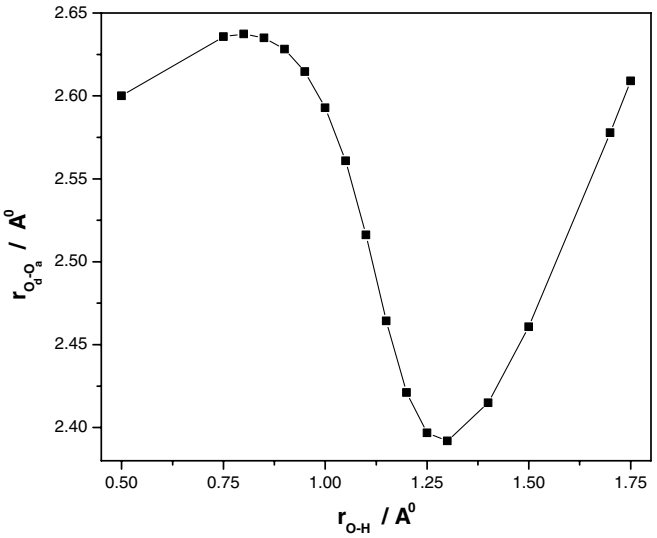

Fig. 3. Variation of $O_d(2')$–$O_a(6')$ distance of 1H2NA with r_{O_d-H} as obtained from DFT-B3LYP(6-31G) level of theory.

In this article we use the "distinguished co-ordinate" approach as proposed by Sobolewski et al. [63], where O_d–H bond distance is varied and rest of the structural parameters are allowed to relax for each choice of r_{O-H}. Maheswari et al. [64] did an extensive theoretical study on salicylic acid and showed that the variation of O_d–H bond length can be used as reaction co-ordinate in order to get some idea about the PE curve for the ground as well as for the excited state proton transfer processes. Catalán et al. [54] also used the similar reaction co-ordinate (r_{O-H}) for the ESIPT processes of some naphthalene derivatives.

3.1. Ground and excited state potential energy curve of 1H2NA

Ground state potential energy curve, as shown in Fig. 5 revels that the enol form (N form) is the most stable one. Surprisingly, there is no shallow minimum for the keto form. The barrier for the enol (N) to keto (T) form is about 6.26 kcal/mole and this is large enough to make any GSIPT under thermal conditions. Again calculated free energy change for the keto enol tautomerization of 1H2NA gives large +ve value (9.201 kcal/mole) and the equilibrium constant obtained from the free energy change i.e 1.7×10^{-6} suggests that the above equilibrium lies towards the enol form. On the basis of the equilibrium constant, the population ratio in the

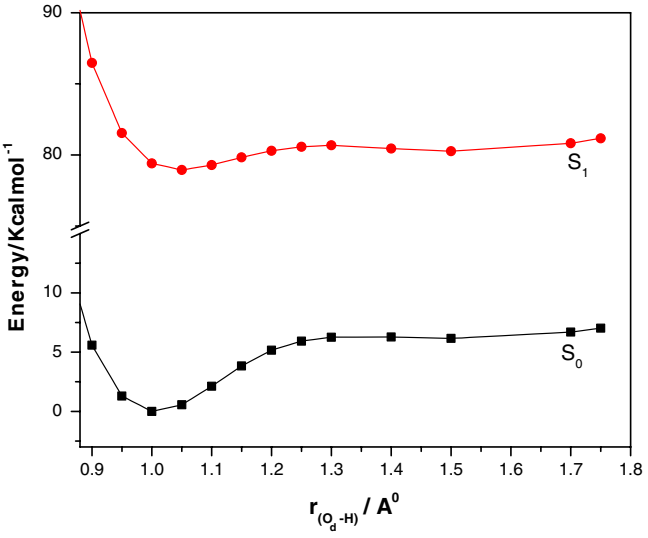

Fig. 5. GSIPT curve (S_0) and ESIPT Franck–Condon curves of 1H2NA as obtained from DFT-B3LYP(6-31G) and TDDFT-B3LYP(6-31G) level of theory.

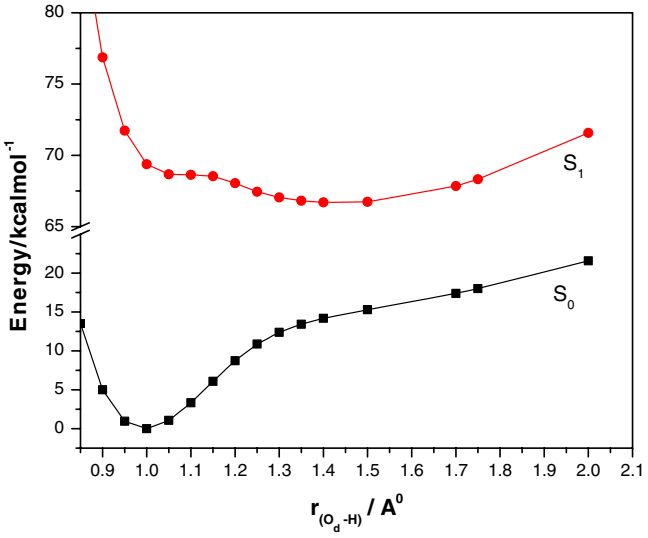

Fig. 6. GSIPT curve (S_0) and ESIPT Franck–Condon curves of 2H3NA as obtained from DFT-B3LYP(6-31G) and TDDFT-B3LYP(6-31G) level of theory.

gas phase for the enol form vs. keto form in the ground state is 6×10^6:1. This again confirms that there is hardly any possibility for GSIPT at normal temperature in 1H2NA.

GSIPT curve for the keto (T) form is almost flat and it implies that the proton transfer fluorescence may not show broad structureless band. Interestingly, in their experimental work Tobita et al. [55] observed a structured and quite less broad emission band of 1H2NA in cyclohexane having $\lambda_{em} \approx 476$ nm. They also observed the red shifted absorption band of 1H2NA is π–π^* in nature with $\lambda_{max} = 368$ nm in cyclohexane. On the other hand, our gas phase calculation shows λ_{max} at 360 nm for the enol (N) form of 1H2NA.Thus our calculated λ_{max} is in good agreement with the experimental findings of Tobita et al.

3.2. Ground and excited state potential energy curve of 2H3NA

For the calculation of the ground state potential energy curve, we used the same technique as before i.e "distinguished co-ordinate" approach as proposed by Sobolewoki et al. [63] and obtain a minima in the PE curve at r_{O-H} distance near about 1 Å and this is due to the 'N' form of 2H3NA. Surprisingly, there is no shallow minimum for the 'T' form, rather the ground state potential energy curve (Fig. 6) increases steadily as the r_{O-H} distance increases from 1 to 2 Å. FC potential energy curve for the S_1 state shows two minima, one at $r_{O-H} \approx 1$ Å and other which is much lower in energy at $r_{O-H} \approx 1.5$ Å. The former is due to the excited enol form (N^*) and the latter minima is due to the excited keto tautomer (T^*). The repulsive nature of the GSIPT curve and the energy gap between the S_0 and S_1 curve at the keto tautomer position ($r_{O-H} \approx 1.5$ Å) implies that the keto tautomer emission will be broad, structureless and largely red shifted. In their laser-induced fluorescence measurements Wu et al. [56] showed a large stokes shifted, extremely weak emission band of 2H3NA maximized at ~715 nm for the keto tautomer resulted from ESIPT. We believe that the nanosecond UV pulse excites the normal species to a vibronic S_1 state vis a Franck–Condon transition where the nuclear co-ordinates remain unchanged. The rapid charge distribution after excitation results in electronic potential surface possessing substantial gradient and an energy minimum shifted towards the proton position in the keto-tautomer. Potential energy surface of the S_1 state shows that some of the normal vibrational modes are displaced from the equilibrium position. As a result, the system begins to evolve along these normal co-ordinates on the excited state energy surface towards a new equilibrium position. This motion may be conceived as the propagation of a wave-packet made up of the superposition of wave functions of various vibronic states that are involved in the temporal development. Especially, those vibrational co-ordinates coupled with the proton displacement should deviate significantly from the equilibrium position, which is eventually reached by the formation of the excited keto tautomer.

The repulsive nature of the ground state PE curve outright discarded the possibility of the ground state intramolecular proton transfer in 2H3NA. Again our free energy calculations for the ground state enol–keto equilibrium of 2H3NA give a positive free energy change ($\Delta G = 29.70$ kcal/mole) and the calculated equilibrium constant is $\sim 1.40 \times 10^{-22}$. On the basis of the equilibrium constant, the population ratio in the gas phase for the enol vs. keto form in the ground state is 7×10^{21}:1. This clearly explain that the GSIPT is thermodynamically unfavorable. Experimental investigations of Wu et al. [56] shows that

λ_{max} of 2H3NA in cyclohexane is nearly 390 nm. On the other hand, our calculated value of λ_{max} in the gas phase is near about 404 nm and this is in good agreement with their experimental findings.

3.3. Comparison of IMHB and ESIPT of 1H2NA and 2H3NA

Both the compound 1H2NA and 2H3NA contain naphthalene ring and two other chromophore –OH and –CHO. But they differ only on the relative position of the –OH and –CHO group. Our calculation suggests that for both of these molecules the 'N' form is the most stable in their ground state. Strength of IMHB is nearly 5 kcal/mole more in 1H2NA than 2H3NA. As far as the ring skeleton of the 'N' form is concerned, 1H2NA and 2H3NA resembles with phenanthrene and anthracene respectively. We then decided to compare the energy of phenanthrene and anthracene using the same quantum mechanical method (DFT/B3LYP with 6-31G basis) and to our utter surprise, we found that energetically phenanthrene is nearly 5 kcal/mole more stable than anthracene.

Fig. 5 shows that the excited singlet i.e, $^1(\pi\pi^*)$ state potential energy curve of 1H2NA has a minima at the equilibrium distance of the N-tautomer and a wide minima with a little depth near the keto tautomer position. Fig. 5 also shows that the barrier of N-tautomer and T-tautomer is very small. If the proton transfer process or any other non-radiative deactivation channel is quite fast compare to the lifetime of excited N-tautomer, as is observed by Tobita et al. [55] for 1H2NA, it will be very difficult to observe the emission from N-tautomer. On the other hand, due to the faster formation rate, population of T-tautomer will be much enough to observe emission. Whereas the $^1(\pi\pi^*)$ potential energy curve of 2H3NA exhibit two minima and an exothermal behavior of the potential energy curve of the T-tautomer explains the occurrence of the proton transfer fluorescence.

A detailed analysis of the electron density of HOMO and LUMO of these two compounds can through some light on the ground and excited states proton transfer processes. Both HOMO and LUMO are of π type, but their phases are quite different in 1H2NA and 2H3NA. The HOMO orbital on the IMHB ring of 1H2NA (Fig. 7) is primarily of bonding character over the C(3′)C(4′)C(5′) atoms, where as C(3′)O(2′) and C(5′)O(6′) show anti-bonding character. Both the hydroxyl oxygen and aldehyde oxygen have bonding character, with a larger electron density over the hydroxyl oxygen. Analysis of the HOMO electron density after the ground state proton transfer (Fig. 8) still shows the larger density on the hydroxyl oxygen and also a shift of electron density over the C(4′)–C(5′) bond. HOMO electron density around the IMHB ring (Fig. 9) of N-tautomer of 2H3NA shows a node at C(4′). Again there is no electron density contribution over the aldehyde group of 2H3NA. HOMO electron

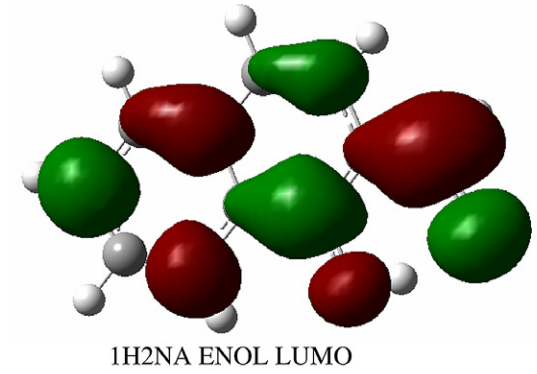

Fig. 7. HOMO and LUMO orbitals of 1H2NA (enol form) as obtained with DFT-B3LYP(6-31G).

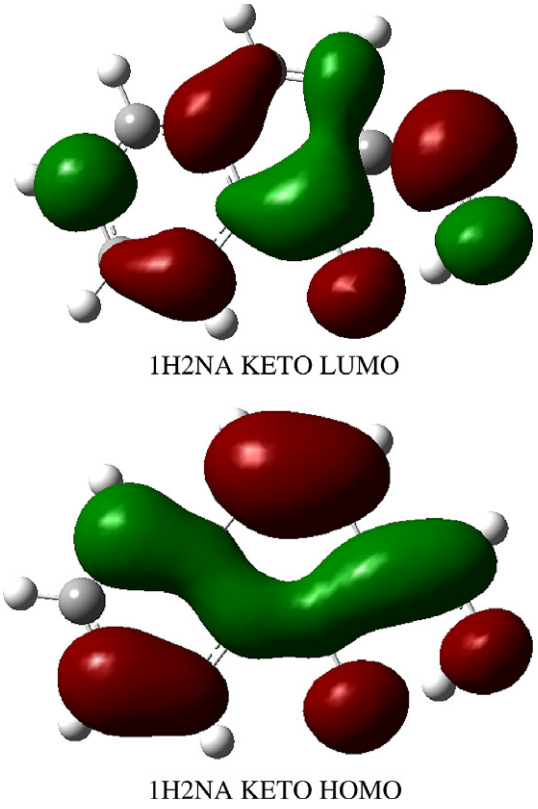

Fig. 8. HOMO and LUMO orbitals of 1H2NA (keto form) as obtained with DFT-B3LYP(6-31G).

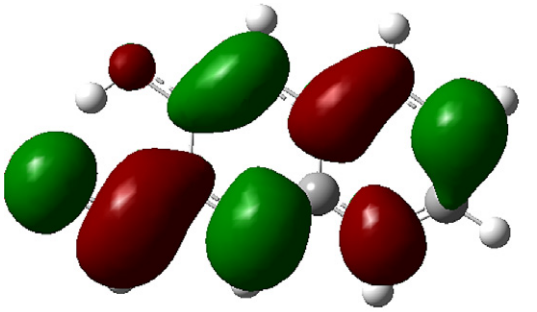

2H3NA ENOL LUMO

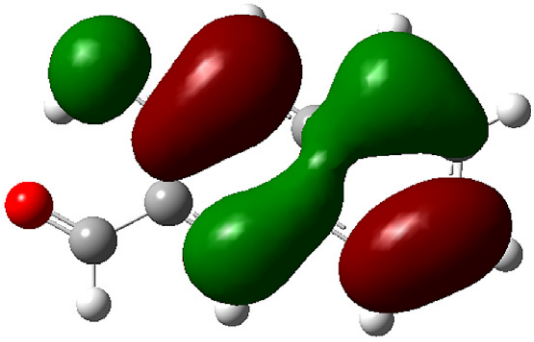

2H3NA ENOL HOMO

Fig. 9. HOMO and LUMO orbitals of 2H3NA (enol form) as obtained with DFT-B3LYP(6-31G).

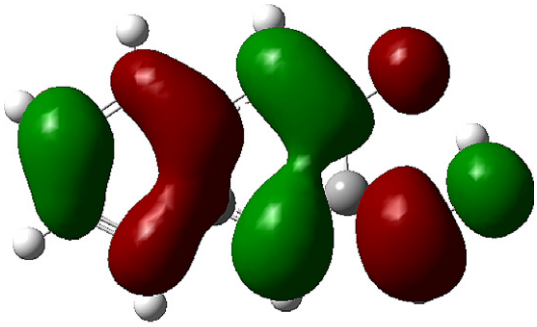

2H3NA KETO LUMO

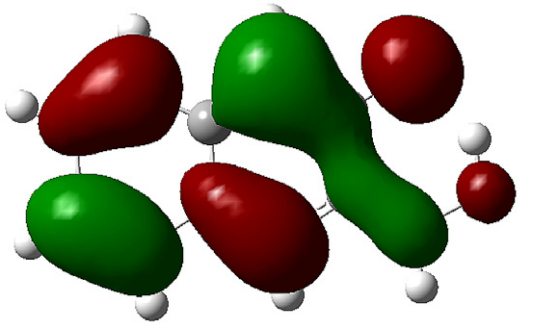

2H3NA KETO HOMO

Fig. 10. HOMO and LUMO orbitals of 2H3NA (keto form) as obtained with DFT-B3LYP(6-31G).

density of the ground state proton transfer form of 2H3NA (Fig. 10) shows less electron density on C(4′)–C(5′) and aldehyde oxygen than that of 1H2NA. Thus the lower conjugation through the IMHB ring in 2H3NA weakens its IMHB strength. Again the less effective electron transfer along the proton transfer co-ordinate makes the GSIPT process less probable. The opposite effect was found for 1H2NA, thereby strengthening the IMHB ring system and stabilizing the GSIPT potential energy curves with respect to 2H3NA. Nevertheless, this stabilization is not sufficient for producing a GSIPT process.

For both 1H2NA (Fig. 7) and 2H3NA (Fig. 9) LUMO is π^* in nature. If we look into the electronic charge distribution of LUMO within IMHB ring (N-tautomer) for both 1H2NA and 2H3NA, C(4′)C(5′) position have bonding character, whereas C(3′)(2′), C(3′)C(4′) and C(5′)O(6′) have antibonding character. The LUMO of the enol form of 2H3NA possess a high electron density on the O(6′) atom and there is no distribution of electron on the O(2′) atom. On the other hand, the LUMO of 1H2NA possess high electron at O(6′) and comparatively low electron density at O(2′) than that of the corresponding HOMO. After tautomerization, the LUMO of the keto-tautomer of 2H3NA still shows high electron density on the O(6′) atom and much lower electron density on the O(2′) atom. Thus it favors the transfer of a proton from O(2′) to O(6′). But in case of keto-tautomer of 1H2NA, both O(2′) and O(6′) has comparable electron density as that of the HOMO. So ESIPT process in 1H2NA is less favorable compare to 2H3NA. Our PES calculations along the proton transfer coordinate also suggest that exothermal behavior of ESIPT processes.

Our PES calculations of 1H2NA suggest that both the ‘N’ and ‘T’ form has comparable energy in the first excited singlet state. We believe, due to the faster rate of formation of the excited ‘T’ form and also the presence of other faster non-radiative deactivation channel from the excited singlet form of N tautomer, it is very difficult to observe normal emission in 1H2NA.

4. Conclusion

For the molecules 1H2NA and 2H3NA, the relative position of the –OH and –CHO group determine the strength of intramolecular hydrogen bond and the nature of ESIPT emission. In the ground state, strength of IMHB in 1H2NA is more compare to 2H3NA. Free energy calculation, HOMO electron density and also ground state PE calculation for both 1H2NA and 2H3NA support the non-viability of GSIPT processes. On the other hand, excited state potential energy and LUMO electron density calculations support the ESIPT for both 1H2NA and 2H3NA. Nature of the ground and excited state potential energy curve nicely explain the red shifted broad structure-less emission band of 2H3NA and also the less broad and less stokes shifted ESIPT band of 1H2NA. Analysis of the LUMO electron density suggests that ESIPT is more favorable in 2H3NA. Since all the calculations have been carried out by DFT method with hybrid

functional (B3LYP/6-31G), it again supports the potentiality of DFT method for the calculations of ESIPT processes.

Acknowledgement

We gratefully acknowledge the financial support received from DST (Ref. No. SR/FTP/PS-60/2003) and UGC, New Delhi for carrying out this research work.

Appendix A. Supplementary data

Supplementary data associated with this article can be found, in the online version, at doi:10.1016/j.theochem.2006.12.010.

References

[1] P.T. Chou, D. MxMorrow, T.J. Aartsma, M. Kasha, J. Phys. Chem. 88 (1984) 4596.
[2] J. Catalan, J.L. Paz, J.C.D. Valle, M. Kasha, J. Phys. Chem. A 198 (1997) 5284.
[3] J. Keck, M. Roessler, C. Schroeder, G.J. Stueber, F. Waiblinger, M. Stein, D. Legourrierec, H.E.A. Kramer, H. Hoier, S. Henkel, P. Fischer, H. Port, T. Hirsch, G. Tytz, P. Hayoz, J. Phys. Chem. A 102 (1998) 6975.
[4] M.L. Martinej, W.C. Cooper, T.T. Chou, Chem. Phys. Lett. 193 (1992) 151.
[5] R.W. Munn, Chem. Br. (1989) 517.
[6] A. Sytnik, M. Kasha, Proc. Natl. Acad. Sci. USA 80 (1980) 8627.
[7] J. Catalan, J.C. Valle, J. Palomar, C. Diaz, J.L.G. Paz, J. Phys. Chem. A 103 (1999) 10921.
[8] T. Nishiya, S. Yamauchi, N. Hirota, Y. Fufiwara, M. Itah, J. Am. Chem. Soc. 108 (1986) 3880.
[9] C. Lu, R.M. Hsieh, L.R. Lee, P.Y. Cheng, Chem. Phys. Lett. 310 (1999) 103.
[10] J.A. Organero, M. Moreno, L. Santos, J.M. Lluch, A. Douhal, Chem. Phys. Lett. 328 (2000) 83.
[11] J.A. Organero, M. Moreno, L. Santos, J.M. Lluch, A. Douhal, J. Phys. Chem. A 104 (2000) 8424.
[12] S. Maheshwari, A. Chowdhury, N. Sathyamurthy, H. Mishra, H.B. Tripathi, M. Panda, J. Chandrasekhar, J. Phys. Chem. A 103 (1999) 6257.
[13] J. Catalan, J. Palomar, J.L.G. Paz, J. Phys. Chem. A 101 (1997) 7914.
[14] S. Nagaoka, Y. Shinde, K. Mukal, U. Nagashima, J. Phys. Chem. A 101 (1997) 3061.
[15] E. Orton, M.A. Morgan, G.C. Pimentel, J. Phys. Chem. 94 (1990) 7936.
[16] P.T. Chou, M.L. Martinez, S.L. Studer, J. Phys. Chem. 95 (1991) 10306.
[17] V. Vargas, L. Amigo, J. Chem. Soc., Perkin Trans. 2 (2001) 1124.
[18] L. Antonov, W.M.F. Fabian, D. Nedltcheva, F.S. Kamounah, J. Chem. Soc., Perkin Trans. 2 (2000) 1173.
[19] S.H. Alarcon, A.C. Olivieri, D. Sanz, R.M. Claramunt, J. Elguero, J. Mol. Struct. 705 (2004) 1.
[20] I.K. Starzomska, A. Filarowski, M. Rospenk, A. Koll, S. Mlikova, J. Phys. Chem. A 108 (2004) 2131.
[21] A. Weller, Z. Elektrochem. 60 (1956) 1144.
[22] A. Weller, Prog. React. Kinet. 1 (1961) 187.
[23] F. Lahmani, A. Zehnacker-Rentien, J. Phys. Chem. A 101 (1997) 6141.
[24] D. Gormin, A. Sytnik, M. Kasha, J. Phys. Chem. A 101 (1997) 672.
[25] P.F. McGarry, S. Jockusch, Y. Fujiwara, N.A. Kaprinidis, N.J. Turro, J. Phys. Chem. A 101 (1977) 764.
[26] V. Guallar, M. Moreno, J.M. Lluch, F. Amat-Guerri, A. Douhal, J. Phys. Chem. 100 (1996) 19789.
[27] J. Keck, H.E.A. Kramer, H. Port, T. Hirsch, P. Fischer, G. Rytz, J. Phys. Chem. 100 (1996) 14468.
[28] F. Parsapour, D.F. Kelley, J. Phys. Chem. 100 (1996) 2791.
[29] R.M. Tarkka, S.A. Jenekhe, Chem. Phys. Lett. 260 (1996) 533.
[30] H. Zhang, P. van der Meulen, M. Glasbeek, Chem. Phys. Lett. 253 (1996) 97.
[31] S. Mitra, R. Das, S.P. Bhattacharyya, S. Mukherjee, J. Phys. Chem. A 101 (1997) 293.
[32] P.G. Yi, Y.H. Liang, C.Z. Cao, Chem. Phys. 315 (2005) 297.
[33] S. Nagaoka, U. Nagashima, J. Phys. Chem. 94 (1990) 1425.
[34] S. Nagaoka, U. Nagashima, Chem. Phys. 136 (1989) 153.
[35] M.V. Verner, S. Scheiner, J. Phys. Chem. 99 (1995) 642.
[36] A.L. Sobolewski, W. Domcke, Chem. Phys. 184 (1994) 115.
[37] J. Catalan, J. Palomar, J.L.G. De Paz, J. Phys. Chem. A 101 (1997) 7914.
[38] K.-Y. Law, J. Shoham, J. Phys. Chem. 98 (1994) 3114.
[39] K.-Y. Law, J. Shoham, J. Phys. Chem. 99 (1995) 12103.
[40] A.U. Acuna, F. Toribio, F. Amat-Guerri, J. Catalan, J. Photochem. 30 (1985) 339.
[41] F. Toribio, J. Catalan, F. Amat, A.U. Acuna, J. Phys. Chem. 87 (1983) 817.
[42] A.U. Acuna, F. Amat-Guerri, J. Catalan, F. Gonzalez-Tablas, J. Phys. Chem. 84 (1980) 629.
[43] J. Goodman, L.E. Brus, J. Am. Chem. Soc. 100 (1978) 7472.
[44] K.K. Smith, K.J. Kaufmann, J. Phys. Chem. 82 (1978) 2286.
[45] S. Nagaoka, N. Hirota, M. Sumitani, K. Yoshihara, J. Am. Chem. Soc. 105 (1983) 4220.
[46] T. Nishiya, S. Yamauchi, N. Hirota, M. Baba, I. Hanazaki, J. Phys. Chem. 90 (1986) 5730.
[47] L.A. Peteanu, R.A. Mathies, J. Phys. Chem. 96 (1992) 6910.
[48] M.A. Morgan, E. Orton, G.C. Pimentel, J. Phys. Chem. 94 (1990) 7927.
[49] S. Nagaoka, N. Hirota, M. Sumitani, K. Yoshihara, E. Lipezynska-Kochany, H. Iwamura, J. Am. Chem. Soc. 106 (1984) 6913.
[50] S. Nagaoka, U. Nagashima, N. Ohta, M. Fujita, T. Takemura, J. Phys. Chem. 92 (1988) 166.
[51] J. Catalan, F. Toribio, A.U. Acuna, J. Phys. Chem. 86 (1982) 303.
[52] E.D. Bergmann, Y. Hirshberg, S. Pinchas, J. Chem. Soc. (1950) 2351.
[53] U.V. Naboikin, B.A. Zadorozhnyi, E.N. Pavlova Opt. Spectrosc.(Eng. Transl.) 6 (1959) 312.
[54] J. Catalán, J.C. del Valle, J. Palomar, C. Di'az, J.L.G. de Paz, J. Phys. Chem. A 103 (1999) 10921.
[55] S. Tobita, M. Yamamoto, N. Kurahayashi, R. Tsukagoshi, Y. Nakamura, H. Shizuka, J. Phys. Chem. A 102 (1998) 5206.
[56] K.C. Wu, Y.M. Cheng, Y.S. Lin, Y.S. Yeh, S.C. Pu, Y.H. Hu, J.K. Yu, P.T. Che, Chem. Phys. Lett. 384 (2004) 203.
[57] A. Bouchy, D. Rinaldi, J.-L. Rivail, Int. J. Quant. Chem. 96 (2004) 273.
[58] A. Dreuw, M. Head-Gordon, Chem. Rev. 105 (2005) 4009.
[59] A.D. Becke, J. Chem. Phys. 98 (1993) 5648;
C. Lee, W. Yang, R.G. Parr, Phys. Rev. B 37 (1988) 785.
[60] V. Barone, C. Adamo, J. Phys. Chem. 99 (1995) 15062.
[61] Gaussian 03, Revision C.02, M. J. Frisch, G. W. Trucks, H. B. Schlegel, G. E. Scuseria, M. A. Robb, J. R. Cheeseman, J. A. Montgomery, Jr., T. Vreven, K. N. Kudin, J. C. Burant, J. M. Millam, S. S. Iyengar, J. Tomasi, V. Barone, B. Mennucci, M. Cossi, G. Scalmani, N. Rega, G. A. Petersson, H. Nakatsuji, M. Hada, M. Ehara, K. Toyota, R. Fukuda, J. Hasegawa, M. Ishida, T. Nakajima, Y. Honda, O. Kitao, H. Nakai, M. Klene, X. Li, J. E. Knox, H. P. Hratchian, J. B. Cross, C. Adamo, J. Jaramillo, R. Gomperts, R. E. Stratmann, O. Yazyev, A. J. Austin, R. Cammi, C. Pomelli, J. W. Ochterski, P. Y. Ayala, K. Morokuma, G. A. Voth, P. Salvador, J. J. Dannenberg, V. G. Zakrzewski, S. Dapprich, A. D. Daniels, M. C. Strain, O. Farkas, D. K. Malick, A. D. Rabuck, K. Raghavachari, J. B. Foresman, J. V. Ortiz, Q. Cui, A. G. Baboul, S. Clifford, J. Cioslowski, B. B. Stefanov, G. Liu, A. Liashenko, P. Piskorz, I.

Komaromi, R. L. Martin, D. J. Fox, T. Keith, M. A. Al-Laham, C. Y. Peng, A. Nanayakkara, M. Challacombe, P. M. W. Gill, B. Johnson, W. Chen, M. W. Wong, C. Gonzalez, J. A. Pople, Gaussian Inc., Wallingford CT, 2004.
[62] I.M. Hunsberger, J. Am. Chem. Soc. 72 (1950) 5626.
[63] A.L. Sobolewski, W. Domcke, Chem. Phys. 232 (1998) 257.
[64] S. Maheshwari, A. Chowdhury, N. Sathyamurthy, H. Mishra, H.B. Tripathi, M. Panda, J. Chandrasekhar, J. Phys. Chem. A 103 (1999) 6257.